Proceedings of International Conference on Aerospace Science and Technology
26-28 June, 2008, Bangalore, India

INCAST 2008-017

Two Dimensional Unsteady Flow over an Open Acoustic Cavity

J. Jaidev Vyas,
PG Student, Thermal Egg Division, National Institute of Technology, Warangal-506004, India
and
Vidyadhar Y. Mudkavi
CTFD Division, National Aerospace Laboratories, Bangalore-560037, India

Abstract

A finite difference code with multi-block capability and based on MacCormack time marching is developed to simulate two-dimensional unsteady compressible viscous laminar flow over an open cavity. The length to depth ratio of the cavity (L/D) is taken to be 4. The flow in the cavity is dominated by vorticity that acts as a source of sound and is transported downstream. The flow Reynolds number based on cavity depth is Re_D =1500 and the Mach number M = 0.15. The radiated sound is further computed using a modified form of the Curle's integral equation in which the source terms are calculated from flow fluctuations. Results show that the wall contributes most to the sound as expected. The code was validated against standard flow problems.

Keywords: Computational Aero Acoustics, Curle's equation, low Mach number, open cavity, noise generation.

1. Introduction

Aeroacoustics, or the sound generated by fluid flows, is an area of research that has received an increasing amount of attention during the past decade. Most of the research has been aimed at high Mach-number applications, with jet noise being the most typical case of interest. The interest for aeroacoustics in the vehicle industry has increased during the last few years, primarily because of customer surveys that show wind noise to be a common complaint [1]. In vehicle applications, the Mach numbers of the flows are typically small (<0.2).

In the present work, flow over an open cavity is studied. This problem can be viewed as a canonical problem for aeroacoustic studies. As a precursor, it is essential to accurately simulate the unsteadiness due to the presence of the cavity. This field is further used to compute the sound field. The acoustic radiation is governed by Lighthill's wave equation [2].

$$\frac{\partial^2 \rho}{\partial t^2} - c_0^2 \frac{\partial^2 \rho}{\partial x_i^2} = \frac{\partial^2 T_{ij}}{\partial x_i \partial x_j}$$

Where $T_{ij} = \rho u_i u_j - \tau_{ij} + (p - c_0^2 \rho)\delta_{ij}$ is called the Lighthill tensor, calculated from the flow solution. c_o is the speed of sound, ρ is the density, t is the time, x is spatial coordinate and δ is the kronecker delta function. Curle solved Lighthill's equation on a bounded domain, where the boundary surfaces are stationary with respect to observer [3].

1.1 Objectives

The objectives of the present work are to

1) Investigate the noise generation process, specifically the noise generation in wall bounded, separated, low Mach-number flows.
2) Simulate the flow field accurately, which is required for the prediction of the acoustic field.
3) Establish major sources of sound.

2. Methodology

A finite difference compressible NS code in two dimensions is developed. The code is first validated against the standard case of channel flow and then its capability is extended to include multi-block. Subsequently, it is applied to an acoustic cavity.

2.1 Governing Equations

The compressible Navier–Stokes equations, written in compact, conservative form are

$$\frac{\partial U}{\partial t}+\frac{\partial E}{\partial x}+\frac{\partial F}{\partial y}=0 \qquad (2)$$

$$\mathrm{U}=\begin{Bmatrix}\rho\\ \rho u\\ \rho v\\ E_t\end{Bmatrix} \qquad (3a)$$

$$\mathrm{E}=\begin{Bmatrix}\rho u\\ \rho u^2+p-\tau_{xx}\\ \rho uv-\tau_{xy}\\ (E_t+p)u-u\tau_{xx}-v\tau_{xy}+q_x\end{Bmatrix} \qquad (3b)$$

$$\mathrm{F}=\begin{Bmatrix}\rho v\\ \rho uv-\tau_{xy}\\ \rho v^2+p-\tau_{yy}\\ (E_t+p)v-u\tau_{xy}-v\tau_{yy}+q_y\end{Bmatrix} \qquad (3c)$$

Here τ is the shear stress, U is the solution vector, E and F are flux vectors, u and v are components of velocity in x and y directions respectively, q_x and q_y are heat fluxes in the respective directions and E_t is the internal energy. Shear and normal stresses are given by stress-strain relationships and heat fluxes are given by Fourier's law of heat conduction.

Along with the above, the equation of state

$$p=\rho RT \qquad (3d)$$

is also solved.

2.2 Numerical Method

In the present work *MacCormack's* time marching technique in finite difference approach is chosen [4]. It is an explicit time marching technique with second order accuracy in both time and space.

It employs a two-step predictor-corrector technique.

Predictor step:

$$\left(\frac{\partial U}{\partial t}\right)^{t}_{i,j}=-\left(\frac{E^{t}_{i+1,j}-E^{t}_{i,j}}{\Delta x}\right)-\left(\frac{F^{t}_{j+1,i}-F^{t}_{j,i}}{\Delta y}\right) \qquad (4)$$

$$\overline{U}^{\,t+\Delta t}_{i,j}=U^{t}_{i,j}+\left(\frac{\partial U}{\partial t}\right)^{t}_{i,j}\Delta t \qquad (5)$$

Corrector step:

$$\left(\overline{\frac{\partial U}{\partial t}}\right)^{t+\Delta t}_{i,j}=-\left(\frac{\overline{E}^{\,t+\Delta t}_{i,j}-\overline{E}^{\,t+\Delta t}_{i-1,j}}{\Delta x}\right)-\left(\frac{\overline{F}^{\,t+\Delta t}_{i,j}-\overline{F}^{\,t+\Delta t}_{i,j-1}}{\Delta y}\right) \qquad (6)$$

By means of Taylor's series expansion,

$$U^{t+\Delta t}_{i,j}=U^{t}_{i,j}+\left(\frac{\partial U}{\partial t}\right)_{av}\Delta t \qquad (7)$$

Where

$$\left(\frac{\partial U}{\partial t}\right)_{av}=\frac{1}{2}\left[\left(\frac{\partial U}{\partial t}\right)^{t}_{i,j}+\left(\overline{\frac{\partial U}{\partial t}}\right)^{t+\Delta t}_{i,j}\right] \qquad (8)$$

Time step (Δt) is based on CFL condition.

2.3 Computational Domain

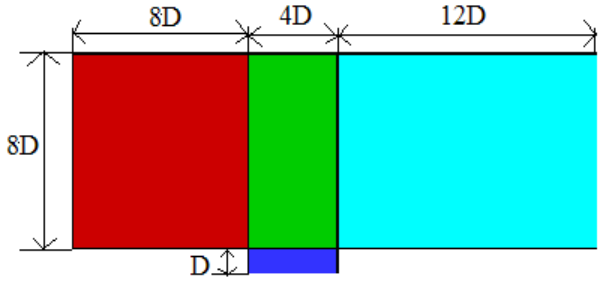

Fig 1: Dimensions are not up to scale

The domain is divided into four blocks as shown above, and "***Multi Block***" logic is incorporated in the code. Information is passed at block boundaries.

3. Radiated Sound Field

Radiated sound field is computed using Curle's integral equation [3]. Curle wrote the solution of the Lighthill's equation as

$$\rho(x,t)-\rho_0=\frac{1}{4\pi c_0^2}\frac{\partial^2}{\partial x_i\partial x_j}\int_V\frac{T_{ij}}{r}dV(y)-\frac{1}{4\pi c_0^2}\frac{\partial}{\partial x_i}\int_S\frac{n_j}{r}(p\delta_{ij}-\tau_{ij})dS(y) \qquad (9)$$

where ρ_0 is the constant of integration, $r=|\boldsymbol{x}-\boldsymbol{y}|$ is the distance between the source and the observer, n_j is the surface normal pointing toward the fluid. The integrands are to be evaluated at the retarded time $\tau=t-r/c_0$.

3.1 Modified Curle's Equation

The spatial derivatives appearing in equation (9) can be replaced with temporal derivatives as shown below

$$\frac{\partial}{\partial x_i}\left[\frac{f(\tau)}{r}\right] = -\frac{\partial r}{\partial x_i}\left[\frac{\dot{f}}{c_0 r} + \frac{f}{r^2}\right] = -l_i\left[\frac{\dot{f}}{c_0 r} + \frac{f}{r^2}\right] \qquad (10)$$

Using the above relationship, equation (9) reduces to

$$p(x,t) - p_0 = \frac{1}{4\pi}\int_V \left[\frac{l_i l_j}{c_0^2 r}\ddot{T}_{ij} + \frac{3l_i l_j - \delta_{ij}}{c_0 r^2}\dot{T}_{ij} + \frac{3l_i l_j - \delta_{ij}}{r^3}T_{ij}\right] dV(y)$$

$$+ \frac{1}{4\pi}\int_S l_i n_j \left[\frac{\dot{p}\,\delta_{ij} - \dot{\tau}_{ij}}{c_0 r} + \frac{p\delta_{ij} - \tau_{ij}}{r^2}\right] dS(y) \qquad (11)$$

where l_i and l_j are components of the unit vector normal to the surface. The detailed explanation of the above derivation is given in reference [4]. As it is confirmed from the literature survey that the wall pressure fluctuations are the major sources of sound, other terms can be neglected to yield the following equation

$$p(x,t) - p_0 = \frac{1}{4\pi}\int_S l_i n_j \left[\frac{\dot{p}\,\delta_{ij}}{c_0 r} + \frac{p\delta_{ij}}{r^2}\right] dS(y) \qquad (12)$$

where a dot denotes time derivative. Since all the faces on the surface contribute to the sound generation

$$p_S(x,t) - p_{0S} = \sum_{faces}\frac{1}{4\pi}\int_{face} l_i n_j \left[\frac{\dot{p}\delta_{ij}}{c_0 r} + \frac{p\delta_{ij}}{r^2}\right] dS(y) \qquad (13)$$

If the source terms and r change only slightly over a face, this can be approximated to

$$p_s(x,t) - p_{o,s} = \sum_{faces}\frac{l_i n_j A_f}{4\Pi}\left[\frac{\dot{p}_f\,\delta_{ij}}{c_o r_c} + \frac{p_f\delta_{ij}}{r_c^2}\right] \qquad (14)$$

where A_f is the face area and r_c is the distance from the observer to the center of the face. The subscript f represents the average value over the face.

4. Results

Computational domain is divided into blocks that are numbered as shown below

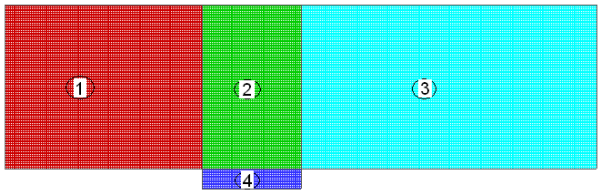

Fig 2: Blocks with Numbering

Computations are carried out with 113×113 grid points in block one, 57×113 grid points in block two, 169×113 grid points in block three and 57×15 points in block four. Grid is uniform in both x and y directions with $\Delta x = \Delta y = 3\times10^{-5}$ m and time step Δt is approximately 5×10^{-8} sec. Depth 'D' of the cavity is calculated from the flow Reynolds number and Mach number, assuming air as the working medium at mean-sea level conditions. Remaining dimensions are calculated from the ratios mentioned in fig.1.

Inlet boundary of block one and top wall boundaries of block one, block two and block three are at flow Reynolds number of Re_D=1500 and at Mach number of M=0.15. No-Slip boundary condition is imposed on bottom wall boundaries of blocks one, block three, block four and on cavity side walls. Properties at the outlet boundary (block three) are extrapolated from the interior domain.

4.1. Flow Features

The flow in open cavities is highly complex and is dominated by vorticity production and transport. Since the geometry is simple, this proves to be an excellent bench mark problem. A sequence of snapshots of instantaneous streamlines is shown in Fig.3.

The sequence shows how the vortices are generated and they move out of the cavity. Here, the time is given in non-dimensional form (tU_∞/D). The sequence of vortex formation and shedding repeats. We choose tU_∞/D=0 as an arbitrary time. The sequence repeats after tU_∞/D=14.40. At the initial instance, there is a primary vortex at left end of the cavity, and just down stream the right wall of the cavity there is another vortex, which is just ejected out of the cavity. At tU_∞/D =4.12 another new vortex is formed at the left wall of the cavity. The new vortex grows in size from tU_∞/D=4.12 to 8.23, pushing the primary vortex to the right end of the cavity. At tU_∞/D=8.23 the free stream fluid starts entering to the cavity. At tU_∞/D =12.35 newly formed vortex dissipates into the free stream. At tU_∞/D= 12.35 another vortex is formed at the left end of the cavity which resembles the primary

vortex formed at initial instance. The primary vortex ejects out of the cavity at tU_∞/D= 14.40.

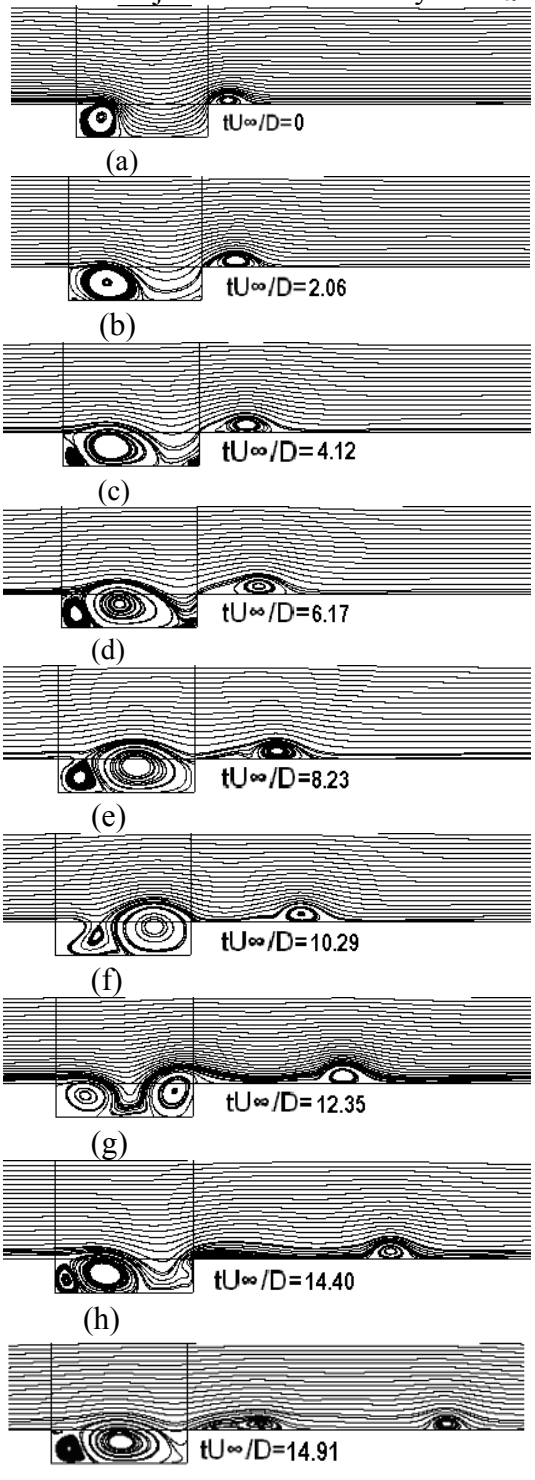

Fig 3: Instantaneous stream lines

This cyclic phenomenon repeats with a non dimensional time period T_p= 14.40. The obtained stream profiles are in good agreement with those given in [5] but the vortices downstream the cavity are little smaller.

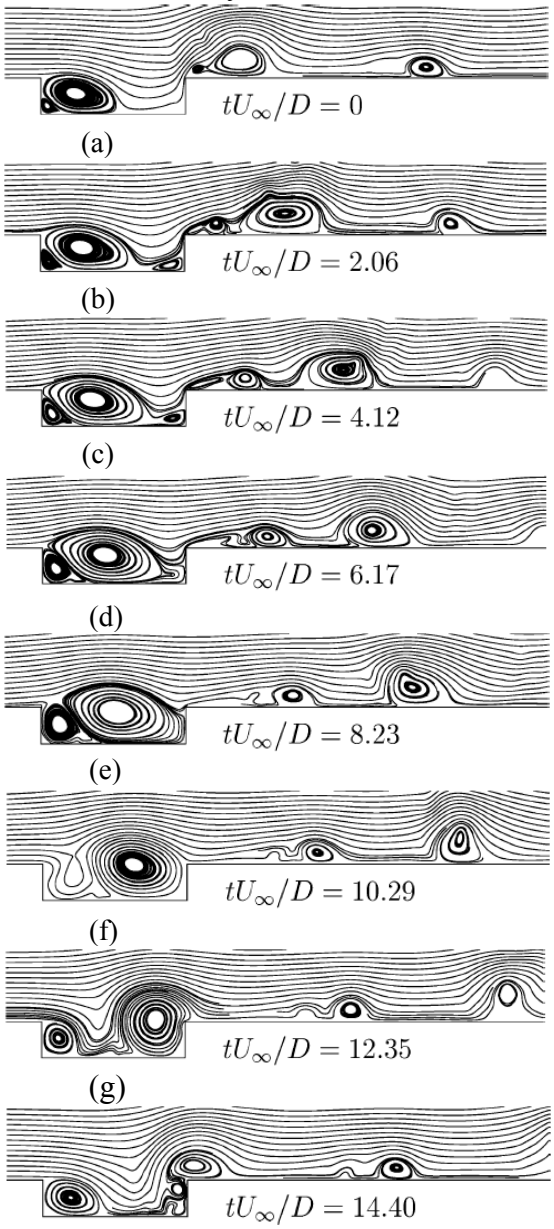

Fig 4: Instantaneous stream lines given in Ref [5]

4.2. Radiated Sound

The radiated sound is calculated at nine observer locations, whose positions are given in table 1.

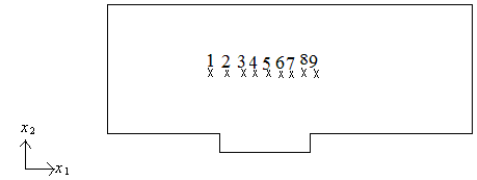

Fig 5: Representation of observer locations

Observer	x_1/D	X_2/D
1	-2	7.16
2	-1	7.16
3	0	7.16
4	1	7.16
5	2	7.16
6	3	7.16
7	4	7.16
8	5	7.16
9	6	7.16

Table 1: observer locations

These points were chosen to match those given in [5].

4.2.1 Sound Pressure Level (SPL)

Since the human ear registers differences in sound levels on a logarithmic scale, it is common to define the Sound Pressure Level as [6].

$$SPL = 20\log_{10}\left(\frac{p'_{rms}}{p_{ref}}\right) \qquad (15)$$

where p'_{rms} is the root mean square value of the pressure fluctuations calculated from equation (14). The sound pressure levels are calculated at the above mentioned nine observer locations and plotted as shown below

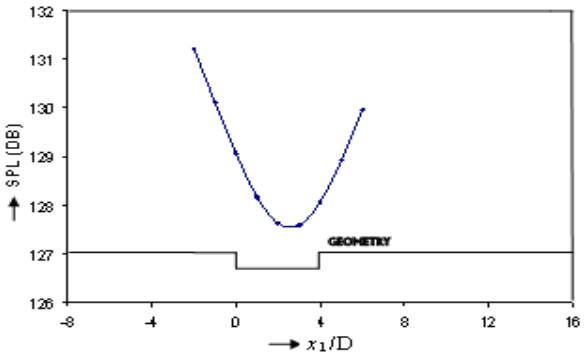

Fig 3. SPL Vs x_1/D

5 Conclusions

A finite difference code is developed to solve two-dimensional compressible unsteady Navier-Stokes equations over an open acoustic cavity. The flow field simulated qualitatively matches the results reported in [5]. The flow in the cavity is dominated by vorticity. The flow achieves a periodic state with continuous production of well-defined coherent vortices in the cavity, which are transported downstream. The vorticity is responsible for the sound generation since the flow is laminar. It is found that maximum sound is radiated towards the upstream of the cavity and that the downstream wall contributes most.

References

1) Larsson, J., *Computational Aero Acoustics for Vehicle Applications*, Licentiate Thesis, Dept. of Thermo and Fluid Dynamics, Chalmers Univ. of Technology, Sweden, Nov. 2002.
2) Sir James Lighthill, *Waves in fluids*, Cambridge University Press, 1987.
3) Curle, N., "The Influence of Solid Boundaries Up on Aerodynamic Sound," *Proceedings of the Royal Society of London*, Vol. A231, 1955, pp. 505–514.
4) John D. Anderson, Jr. *Computational Fluid Dynamics, The basics with applications*, McGraw-Hill, Inc., International Edition, 1995.
5) Johan Larsson, Lars Davidson, Magnus Olsson and Lars-Erik Eriksson. "Aeroacoustic Investigation of an Open cavity at Low Mach Number", *AIAA Journal*, vol. 42, No. 12, December 2004.
6) Hirschberg and S. W. Rienstra. *An Introduction to Aeroacoustics,* Eindhoven University of Technology, 2004.
7) J. Anthoine and C. Schram. "Advances in Aeroacoustics", Lecture series 2001-02, Von Karman Institute, Belgium, March 2001.
8) M. Yousuff Hussaini. *Collected papers of Sir James Lighthill,* Volume III, Oxford University Press, 1997.